EPJ Web of Conferences **2**, 06004 (2010)
DOI:10.1051/epjconf/20100206004

Neutron-induced fission cross sections of short-lived actinides with the surrogate reaction method

B. Jurado[1,a], G. Kessedjian[1], M. Petit[1], M. Aïche[1], G. Barreau[1], A. Bidaud[1], S. Boyer[1], N. Carjan[1], S. Czajkowski[1], D. Dassie[1], C. Grosjean[1], A. Guiral[1], B. Haas[1], D. Karamanis[1], L. Mathieu[1], S. Misicu[1], C. Rizea[1], F. Santiamon[1], L. Audouin[2], N. Capellan[2], L. Tassan-Got[2], J.N. Wilson[2], S. Andriamonje[3], E. Berthoumieux[3], E. Bouchez[3], F. Gunsing[3], A. Hurstel[3], Y. Lecoz[3], R. Lucas[3], Ch. Theisen[3], O. Serot[4], E. Bauge[5], A. Billebaud[6], L. Perrot[6], I. Ahmad[7], J.P. Greene[7], and R.V.F. Janssens[7]

[1] CENBG, Chemin du Solarium B.P. 120, 33175 Gradignan, France
[2] IPN, Univ. Paris-Sud, 91405 Orsay, France
[3] CEA Saclay, DSM/DAPNIA/SPhN, 91191 Gif-sur-Yvette cedex, France
[4] CEA Cadarache, DEN/DER/SPRC/LEPh, 13108 Saint Paul lez Durance, France
[5] CEA DAM DIF, 91297 Arpajon, France
[6] LPSC, 38026 Grenoble cedex, France
[7] Physics Division, Argonne National Laboratory, 9700 S. Cass Avenue, IL 60439, USA

Abstract. We present a review of the fission cross section measurements made by the CENBG collaboration over the last years using the surrogate reaction method. For example the neutron-induced fission cross sections of ^{233}Pa($T_{1/2}$=27 d), ^{242}Cm($T_{1/2}$=162.8 d) and ^{243}Cm($T_{1/2}$=29.1 y) have been obtained by our group with this technique. The advantages and the difficulties of the surrogate method are discussed. Special attention is paid to the comparison between cross sections measured with the surrogate method and those obtained directly with neutrons at low energies. This comparison provides information on possible differences between the spin-parity distributions achieved in the two methods.

1 Introduction

The CENBG collaboration measures nuclear data of interest for the development of the Th fuel cycle and for minor actinides incineration. In both cases there is a big lack of data for short-lived actinides. The direct measurement of cross sections of short-lived nuclei is extremely complicated due to the high radioactivity of the targets [1]. These difficulties can be overcome with the so-called surrogate reaction technique, developed in the 1970's by Cramer and Britt [2]. It consists in measuring the decay probability of a compound nucleus (e.g., fission, neutron emission, or radiative capture) produced via an alternative (surrogate) reaction, in this case we use a few-nucleon transfer reaction. The surrogate reaction is chosen such that the resulting nucleus has the same mass A and charge Z as the compound nucleus (CN) that results in the "desired" neutron-induced reaction. The neutron-induced cross section of nucleus A for decay channel "i" σ_A^i is then deduced from the product of the measured probability P_{exp}^i and the CN cross section for the neutron-induced reaction obtained from optical model calculations σ_{A-1}^{CN} :

$$\sigma_A^i = P_{exp}^i \sigma_{A-1}^{CN} \quad (1)$$

In this contribution, we focus on fission cross section measurements. Thus, the exit channel of the surrogate reaction consists of a light ejectile and fission fragments.
An important issue to be investigated in the context of surrogate reactions is the difference between the distributions in spin and parity ($J\pi$) of the states populated in the desired and surrogate reactions, a problem referred to as the $J\pi$ population mismatch in the literature [3],[4]. Since the $J\pi$ population influences the decay probabilities of the CN, one would expect differences between the decay probabilities measured in surrogate and in neutron-induced experiments. However, in the Weisskopf-Ewing limit, the decay probability is independent of the spin and parity of the CN and eq. 1 is valid. The conditions under which the Weisskopf-Ewing limit applies have been investigated in Refs. [3],[4]. It was stated in Ref. [3] that this limit holds when (i) the excitation energy is sufficiently high for the decay widths to be dominated by the statistical level density, and when (ii) the angular momentum of the CN is not much larger than the spin-cutoff parameter of the level density distribution, which, for the actinide region, is about $7\hbar$. Clearly, the comparison between cross sections measured with the surrogate method and those obtained directly with neutrons at low energies should provide information on possible differences between the $J\pi$ distributions achieved in the two methods. Indeed, at the lowest energies corresponding to the fission threshold, this mis-

[a] e-mail: jurado@cenbg.in2p3.fr

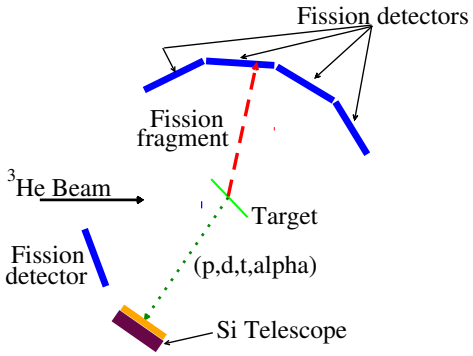

Fig. 1. Top view of the set-up for fission probability measurements.

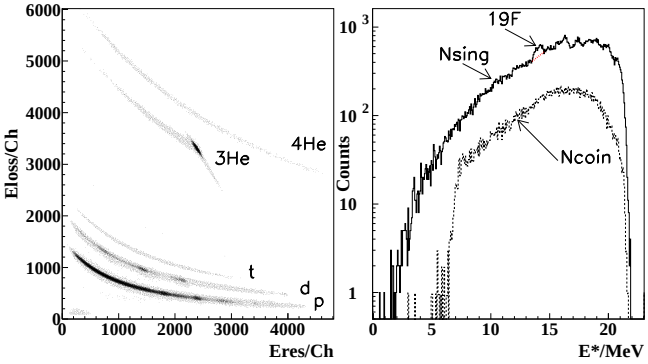

Fig. 2. Left: Energy loss versus residual energy in one of the Si telescopes. Right: Number of tritons as a function of the CN excitation energy. The interpolation of the singles spectrum under the ^{19}F contaminant peaks is represented by the red dotted line (see text for details).

match could be revealed by transition states near the top of the fission barriers whose feeding could be dependent of the entrance channel. The greatest effect is expected for even-even heavy systems which cross the fission barriers through a few collective states. Nevertheless, and because of a larger density, these transition states should be less important for odd-odd systems. Discrepancies between surrogate and neutron-induced data have been attributed to the Jπ population mismatch in Refs. [5],[4].

We perform our measurements at the Tandem accelerator at the IPN Orsay. We use a ^{3}He beam with energies of 24 or 30 MeV. The set-up used to determine the fission probability of the compound nuclei formed after a transfer reaction is displayed in Fig. 1. Two Si telescopes, placed at 130° (angular aperture 4°) with respect to the beam axis, serve to identify the ejectiles. If the corresponding heavy residue undergoes fission, one of the fragments is detected in coincidence by means of a fission-fragment multi-detector consisting of 15 photovoltaic cells distributed among 5 units, each composed of 3 cells placed vertically above one another. Four units provide an angular coverage of 14 to 125°. The fifth unit is positioned at 180° from the foremost unit. In this way, the fission fragments hitting the foremost unit are detected in coincidence with their complementary fragment in one of the cells of the fifth one. The determination of the kinetic energies of the two fragments in a given fission event provides a means to infer the fragment mass distribution [6]. The fifth unit also provides a data point at backward angles for the angular distribution. More details on the experimental set-up can be found in Ref. [7]. This set-up allows determining the fission probability in the following way: The identification of the light charged particles and the determination of their energy and scattering angle is achieved in the Si telescopes. With this information and the related Q-values, the excitation energy E* of the corresponding compound nucleus is determined. The left pannel of Fig. 2 illustrates the identification achieved in one of the telescopes through the conventional energy loss vs residual energy plot. By selecting one type of light particle, for example tritons t, the spectrum represented by the solid line on the right of Fig. 2, the so-called "singles" spectrum N_{sing}, is obtained. It represents the number of tritons, i.e., the number of compound nuclei, as a function of their excitation energy. The broad peaks at the highest excitation energies in the spectrum stem from transfer reactions on the carbon backing of the target and on ^{19}F target inpurities. The background from reactions on carbon is measured separately and subtracted from the singles spectrum. The resulting singles spectrum is interpolated under the ^{19}F impurity peak, introducing an additional source of uncertainty. This systematic error represents at most a 4% contribution to the overall uncertainty. By selecting the tritons detected in coincidence with a fission event, the spectrum associated with the number of compound nuclei that have undergone fission, N_{coin} is obtained (see dashed line in the right pannel of Fig. 2). The ratio between the N_{coin} and N_{sing} spectra, corrected for the fission detector efficiency Eff(E*), gives the fission probability of the CN as a function of the excitation energy, i.e., $P_f(E*) = N_{coin}(E*)/(N_{sing}(E*) \cdot Eff(E*))$. The geometrical efficiency of the fission detector is approximately 47%, and is calculated with a Monte-Carlo simulation that also reproduces the experimental efficiency determined with a ^{252}Cf source. With this Monte-Carlo simulation it is possible to calculate the effective efficiency for each E* bin. The effect of the fission-fragment angular anisotropy on the detector efficiency amounts to at most a 2-3% correction.

2 Results

2.1 Fission cross sections for Pa isotopes

In the first surogate experiment of the CENBG collaboration the surrogate reaction ^{3}He + ^{232}Th $\rightarrow$ p + ^{234}Pa was used to obtain the fission cross section of ^{233}Pa [7]. This nucleus plays a very important role in the Th cycle. Notice the half life of the ^{232}Th target of $1.4 \cdot 10^{10}$ years compared to the 27 days half life of ^{233}Pa. At the moment of the experiment, no fission cross section data existed for this nucleus. The ^{3}He-induced transfer reactions on the ^{232}Th target lead to the production of various heavy residues. Table

Table 1. Transfer channels investigated in the reaction ^{3}He+^{232}Th and the corresponding neutron-induced fission reactions.

Transfer channel	Neutron-induced reaction
^{232}Th(^{3}He,p)^{234}Pa	^{233}Pa(n,f)
^{232}Th(^{3}He,d)^{233}Pa	^{232}Pa(n,f)
^{232}Th(^{3}He,t)^{232}Pa	^{231}Pa(n,f)
^{232}Th(^{3}He,α)^{231}Th	^{230}Th(n,f)

1 lists the different transfer channels considered and the corresponding neutron-induced reactions that can, hence, be obtained with the surrogate method. The advantage of using transfer reactions is clear: the simultaneous access to several transfer channels allows one to determine cross sections for various nuclei from a single projectile-target combination. Moreover, since there are two bodies in the outgoing reaction channel, the excitation energy of the heavy nucleus follows a broad probability distribution. The CN excitation energy E* is related to the neutron energy E_n via the relation $E^* = B_n + (A-1)\cdot E_n/A$, where B_n is the neutron binding energy in the CN. Therefore, for a fixed beam energy, the surrogate method enables the determination of cross sections over a wide range of corresponding neutron energies. In a direct neutron measurement with a monoenergetic neutron beam one we would have needed 4 different targets and several beam energies. Moreover, compared to neutron measurements, surrogate experiments profit from the high intensities of light charged particle beams which reduce considerably the beam time requirements and permit the use of thin targets. The measured fission probabilities are translated into the associated neutron-induced fission cross sections by multiplying the experimental fission probability with the corresponding calculated CN cross section, as indicated by eq. 1. The latter was obtained with a Lane-consistent semi-microscopic [8] deformed [9] optical model potential built using deformed radial nuclear densities calculated in the Hartree-Fock-Bogoliubov framework with the Gogny D1S interaction [10]. The error associated with the CN cross section is about 10%. Fig. 3 shows the fission cross section of ^{231}Pa obtained from the analysis of the triton channel (see table 1). The CENBG data are shown in comparison with the neutron-induced data by Plattard et al. [11] and by Oberstedt et al. [12]. The lines represent the international evaluations. There is good agreement between the three sets of data at the fission threshold. Between 0.8 and 1.5 MeV our data agree better with those of Plattard et al. Above 1.5 MeV our data are below those of Plattard et al. and in agreement with Oberstedt et al. Our data are shifted with respect to Plattards data at the threshold of the second chance fission in agreement with ENDF. Fig. 4 illustrates our results for ^{233}Pa obtained from the analysis of the proton transfer channel (see table 1) compared with the neutron-induced data by Tovesson et al. [13]. Again we find a very good agreement between the surrogate results and the neutron-induced data at the fission threshold. Concerning the international evaluations, in general ENDF is in better agreement with our data than JENDL. In the first plateau between 1.5 and 5.5

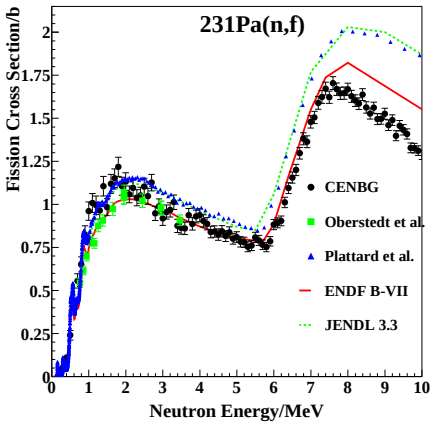

Fig. 3. Fission cross section of ^{231}Pa as a function of neutron energy in comparison with available neutron-induced data and with the evaluations from several international libraries.

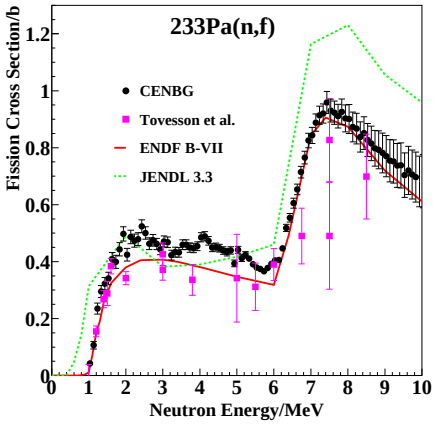

Fig. 4. Fission cross section of ^{233}Pa as a function of neutron energy.

MeV ENDF is lower than our data. For $E_n > 6$ MeV ENDF is in good agreement with our data.

2.2 Fission cross sections for Cm and Am isotopes

The aim of the second fission surrogate experiment was to determine the neutron-induced fission cross sections of ^{242}Cm($T_{1/2}$=162.8d), ^{243}Cm($T_{1/2}$=29.1y) and ^{241}Am($T_{1/2}$ = 432.2y). These cross sections are of interest for nuclear waste transmutation. However, in the case of the Cm isotopes, the available data are rather scarce or inconsistent and the international evaluations present important differences. To attain these nuclei we have employed few-nucleon transfer reactions using a ^{3}He projectile on a ^{243}Am(7370 y) target. Two targets, of approximately 100 $\mu g/cm^2$ thickness, were prepared at the Argonne National Laboratory, each deposited on a 75 μg/cm^2 carbon backing. Table 2 lists the different transfer channels analysed in this experiment. The same set of nuclei was investigated in the

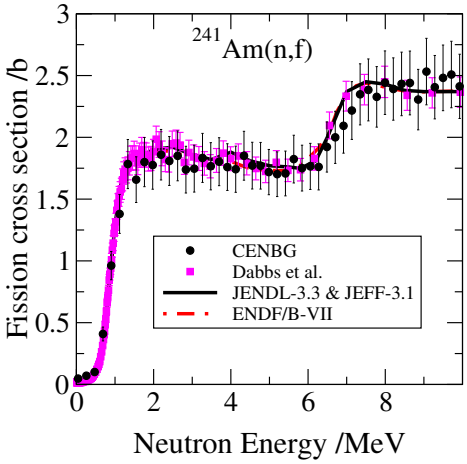

Fig. 5. Fission cross section of ^{241}Am as a function of neutron energy.

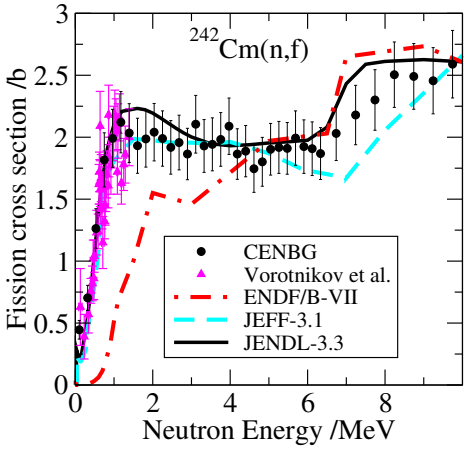

Fig. 6. Fission cross section of ^{242}Cm as a function of neutron energy.

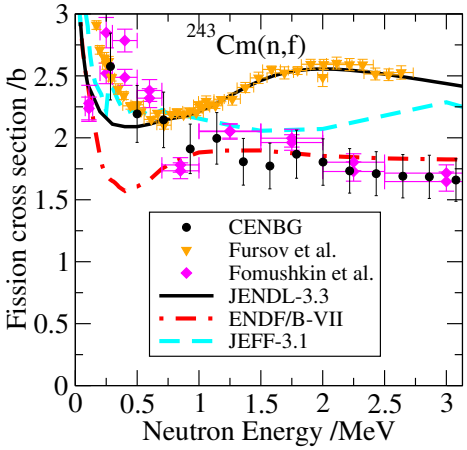

Fig. 7. Fission cross section of ^{243}Cm as a function of neutron energy.

Table 2. Transfer channels investigated in the reaction ^{3}He+^{243}Am and the corresponding neutron-induced fission reactions.

Transfer channel	Neutron-induced reaction
^{243}Am(^{3}He,d)^{244}Cm	^{243}Cm(n,f)
^{243}Am(^{3}He,t)^{243}Cm	^{242}Cm(n,f)
^{243}Am(^{3}He,α)^{242}Am	^{241}Am(n,f)

pioneering work of Gavron et al. [14]. However, the aim of that measurement was the extraction of fission barrier heights and curvatures from the onset of the measured fission probabilities rather than the determination of neutron-induced fission cross sections.

The final error on the reported cross sections is 11% on average and reaches 14% in regions with low statistic. As shown in Fig. 5, the ^{241}Am(n,f) cross section is in good agreement with the data by Dabbs et al. [15] and with the evaluations. Fig. 6 presents the results for ^{242}Cm(n,f) in comparison with the data by Vorotnikov et al. [16]: there is good agreement between both sets. For neutron energies larger than 1.4 MeV, no other experimental data exist. This presumably accounts for the important discrepancies between evaluations based on various international libraries in this energy range, although JENDL and JEFF present the best overall agreement with the data. The ^{243}Cm(n,f) cross section can be found in Fig. 7. Due to the presence of contaminant peaks, the maximum neutron energy shown in this case is 3 MeV. The results are compared with the most recent measurements by Fomushkin et al. [17] and by Fursov et al. [18]. At the lowest neutron energies, the agreement between the three measurements is rather satisfactory. Beyond 0.7 MeV, however, the present data follow those of Ref. [17] fairly well, but they clearly deviate from those of Ref. [18]. Concerning the libraries, JENDL closely follows Ref. [18] above 0.7 MeV. ENDF is in satisfactory agreement with the present data above 0.7 MeV and JEFF is compatible with our data and Ref. [17] only between 0.5 and 1.8 MeV. The cross sections of Ref. [18], in the 1 to 3 MeV energy range, are significantly higher than those measured for neighboring fissile isotopes such as ^{245}Cm [19],[20] and ^{247}Cm [18], which are all below 2 barns. Moreover, under the reasonable assumption that the neutron inelastic scattering cross section of ^{243}Cm ranges from 1 to 1.5 barns at 2 MeV neutron energy, the value of the fission cross section of 2.6 barns obtained in Ref. [18] at 2 MeV would result in a total compound cross section (neglecting the capture contribution) varying from 3.6 to 4.1 barns, a value considerably larger than the 3 barns predicted by optical model calculations [8],[9]. All these arguments suggest that the results in Ref. [18] (and, hence, the JENDL evaluation) overestimate the ^{243}Cm(n,f) cross section at neutron energies between 0.7 MeV and 3 MeV.

2.3 Fission threshold

The previous five figures show that our data reproduce very well the general trend of the neutron cross sections and no

systematic discrepancies are observed between the present results and the neutron-induced measurements at the lowest energies. This good agreement is particularly interesting in the case of the even-odd ^{243}Cm and even-even ^{244}Cm compound nuclei, as it indicates that the Jπ distributions of the states populated through the transfer reactions used in this work are similar to those of the levels fed in the corresponding neutron-induced reactions. This absence of Jπ effects is at variance with the Jπ distribution disparities suggested for CN ^{237}U in Ref. [5], and with Ref. [4] where the Jπ distribution populated in the ^{234}U(t,p) reaction was corrected in order to reproduce the ^{235}U(n,f) data. Note, however, that the fissioning nuclei considered in Refs. [5],[4] are lighter than the ones studied in this work.

3 Perspectives: Fission studies at ELISe

Most of the fission surrogate experiments done up to now are limited to the measurement of cross sections. Although, as mentioned above, our set-up also allows to determine the fission fragment mass distributions with a resolution of 2-3 mass units [6]. A big step on the way to more complete surrogate experiments has been done at GANIL where transfer-induced fission of a ^{238}U beam on a carbon target has been studied [21]. The coupling of inverse kinematics with the large acceptance VAMOS spectrometer has enabled the identification in Z and A of the fission fragments. Outstanding surrogate experiments on fission will be possible at the ELISe facility of the FAIR project. ELISE is a electron-radioactive ion colider [22]. A dedicated set-up for fission studies will be installed, this project is called Fission-at-ELISE (FELISE) [23]. The radioactive ions of interest for fission studies are generated by fragmentation from a ^{238}U primary beam. Long isotopic chains of elements ranging from Ac to Np will be produced. The interaction between the electrons and the radioactive ions occurs through the exchange of virtual photons. After the interaction, the electron is inelastically scattered and the excited heavy ion moves further at relativistic energies and may fission. Therefore, in this case the surrogate reaction is electron inelastic scatering. As in any surrogate experiment, the measurement of the energy of the scattered electron leads to the E* of the CN, and the fission probability can be obtained by dividing the electron-ion coincidences by the total number of scattered electrons. In the ELISe facility the momentum of the electrons is determined with a dedicated spectrometer. Therefore, contrary to all the surrogate experiments performed up to now, it will be possible to determine the angular momentum transferred to the fissioning nucleus and to have a direct knowledge of the populated Jπ parity distribution. In addition, a neutron wall will be installed to measure the neutron multiplicity of each fission fragment. To resume, the FELISE facility offers many advantages: (i) The E* of the fissioning nucleus and the angular momentum transfered in the reaction can be measured. (ii) The interaction of virtual photons with the ions leads to an E* spectrum that corresponds to E_n=0-20 MeV, a domain of interest for reactor physics. (iii) Fission studies of very short-lived nuclei for which no target exists will be possible. (iv) In addition to the fission probabilities, and thanks to the high kinetic energy of the fissioning nucleus, the fission fragments will be unambigously identified in A and Z, and the number of neutrons emitted by each fragment will be measured.

4 Conclusions

The surrogate reaction method was used to determine the neutron-induced fission cross sections of several short-lived actinides. We measured for the first time the fission cross section of ^{233}Pa. Our results for ^{231}Pa(n,f) revealed that the existing neutron-induced data overestimated the fission cross section above 1.5 MeV. The deduced ^{241}Am(n,f) and ^{242}Cm(n,f) cross sections agree with the available data obtained via neutron-induced reactions. The new results for the fission cross section of ^{242}Cm extend up to the onset of second-chance fission. None of the existing neutron-induced fission data for ^{242}Cm reached as high in neutron energy. For the ^{243}Cm(n,f) cross section, the present results are in good agreement with the existing neutron-induced data at the lowest neutron energies, but are clearly below the recent data of Fursov et al. [18] beyond 0.7 MeV. The good agreement observed at the lowest neutron energies between the present results and the neutron-induced data for ^{242}Cm(n,f) and ^{243}Cm(n,f) indicates that the population of excited states generated by the transfer reactions used in this work is similar to the distribution fed in neutron-induced reactions. This agreement illustrates the potential of the surrogate reaction method to provide neutron-induced fission cross sections for short-lived nuclei. Further experimental and theoretical efforts are, however, required to extend the use of this powerful technique to other types of cross sections such as radiative capture as well as to asses and understand the limits of its application. Next generation surrogate experiments on fission will be possible with the project ELISe at the FAIR facility. The main advantages of this facillity with respect to previous surrogate experiments is that the angular momentum transferred will be known. In addition, not only fission probabilities but also total resolution isotopic yields and their correlations with the emitted prompt neutrons will be measured for a wide range of nuclei going from Ac to Np isotopes.

We thank the tandem accelerator staff and the target laboratory of the IPN Orsay for their support during the experiment. This work was partly supported by the CNRS program PACEN/GEDEPEON, the Conseil Régional d'Aquitaine, the U.S. Department of Energy, Office of Nuclear Physics, under contract DE-AC02-06CHII-357. The authors are also indebted for the use of ^{243}Am to the Office of Basic Energy Sciences, U.S. Department of Energy, through the transplutonium element production facilities at Oak Ridge National Laboratory.

References

1. B. Jurado et al., Nucl. Instr. Meth. A (2009), doi:10.1016/j.nima.2009.09.071

2. J. Cramer and H. Britt, Nucl. Sci. Eng. **41**,(1970) 177
3. J. Escher and F. S. Dietrich., Phys. Rev. C **74**,(2006) 054601
4. W. Younes and H. C. Britt, Phys. Rev. C **67**, (2003) 024610
5. B. F. Lyles et al., Phys. Rev. C **76**, (2007) 014606
6. B. Jurado et al., Conf. Proccedings of CNR*2007, California 2007, p.90
7. M. Petit et al., Nucl. Phys. A **735**, (2004) 345
8. E. Bauge, J.P. Delaroche, M. Girod, Phys. Rev. C **63**, (2001) 024607
9. E. Bauge, et al., Phys. Rev. C **61**, (2000) 034306
10. J.F. Berger, et al., Comput. Phys. Commun. **63**, (1991) 365
11. S. Plattard, et al., Phys. ReV. Lett. **46**, (1981) 633
12. S. Oberstedt, et al. Ann. Nucl. Energy **32**, (2005) 1867
13. F. Tovesson et al., Nucl. Phys. A **733** (2004) 3
14. A. Gavron et al., Phys. Rev. C **13**, (1976) 2374
15. J. W. T. Dabbs et al., Nucl. Sci. Eng. **83**, (1983) 2
16. P. E. Vorotnikov et al., Yadern. Fiz. **40**, (1984) 1141
17. E. F. Fomushkin et al., At. Energ. **69**, (1990) 258
18. B. I. Fursov et al., Conf. Nucl. Data for Sci. and Techn., Trieste 1997, p.488
19. E. F. Fomushkin et al., At. Energ. **63**, (1987) 242
20. R. M.White et al., Conf. Nucl. Data for Sci. and Techn., Antwerp 1982, p.218
21. X. Derkx, F. Rejmund et al., this issue
22. H. Simon et al. Nucl. Phys. A 787 (2007) 102
23. J. Taieb et al., Int. Jour. of Mod. Phys. E, 18 (2009) 767